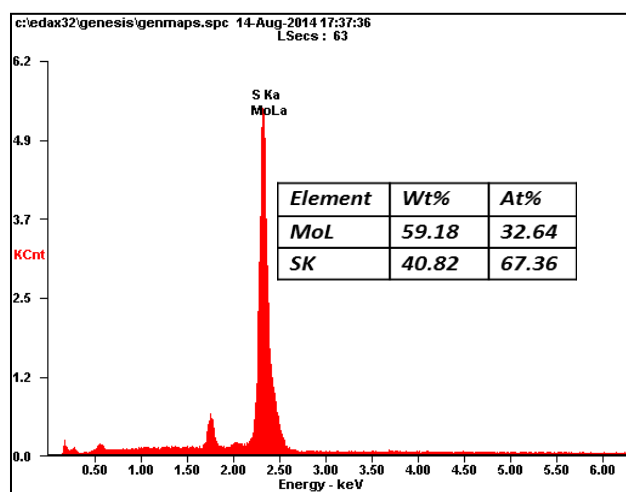
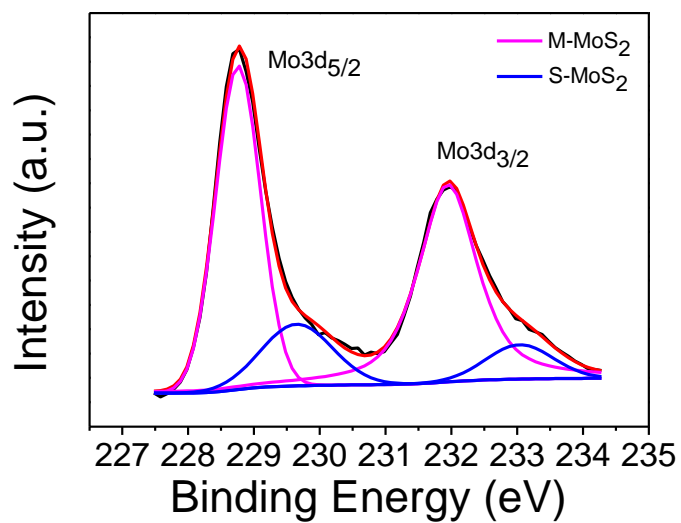


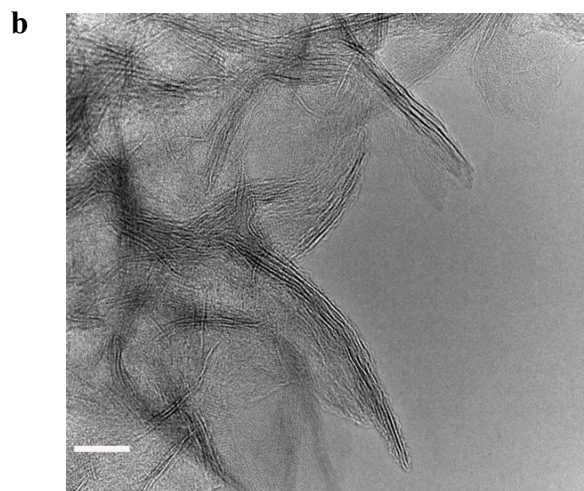
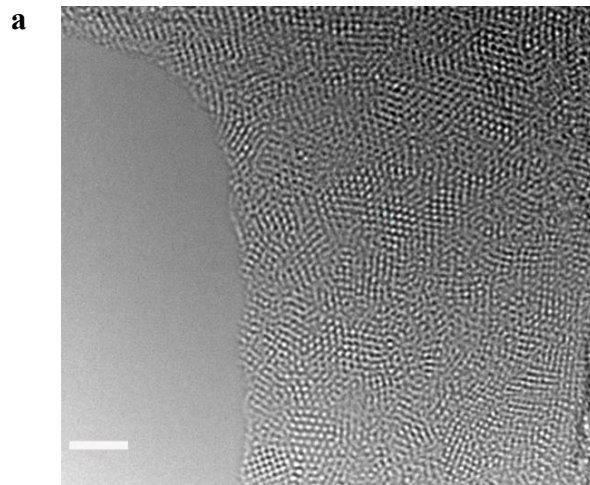
**Supplementary Figure 1: SEM image of S-MoS<sub>2</sub>. Scale bar, 100 nm.** The morphology of S-MoS<sub>2</sub> is similar to that of M-MoS<sub>2</sub> at the nanoscale as shown by SEM images at high magnification.



**Supplementary Figure 2: EDX of M-MoS<sub>2</sub>.** The as-prepared M-MoS<sub>2</sub> was characterized by energy dispersive x-ray spectroscopy (EDX). The atomic ratio of S to Mo was calculated to be around 2.05.

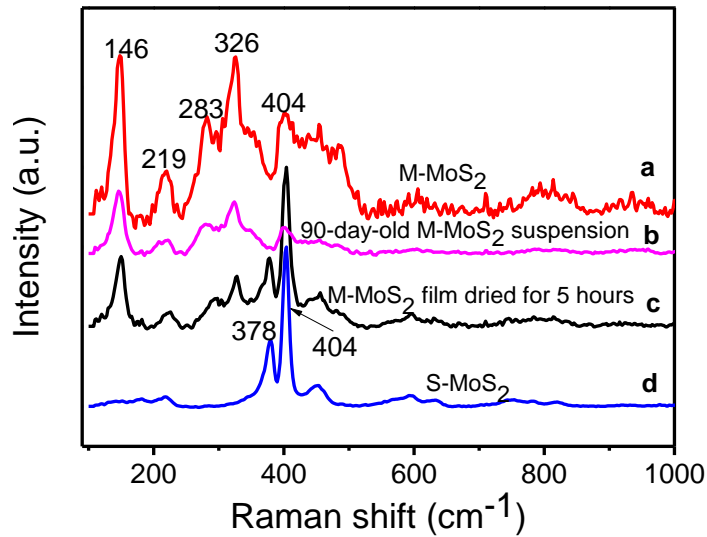


**Supplementary Figure 3: XPS of M-MoS<sub>2</sub>.** After Shirley background subtraction, the Mo 3d peaks were de-convoluted to show the M-MoS<sub>2</sub> (pink) and S-MoS<sub>2</sub> (blue) contributions.

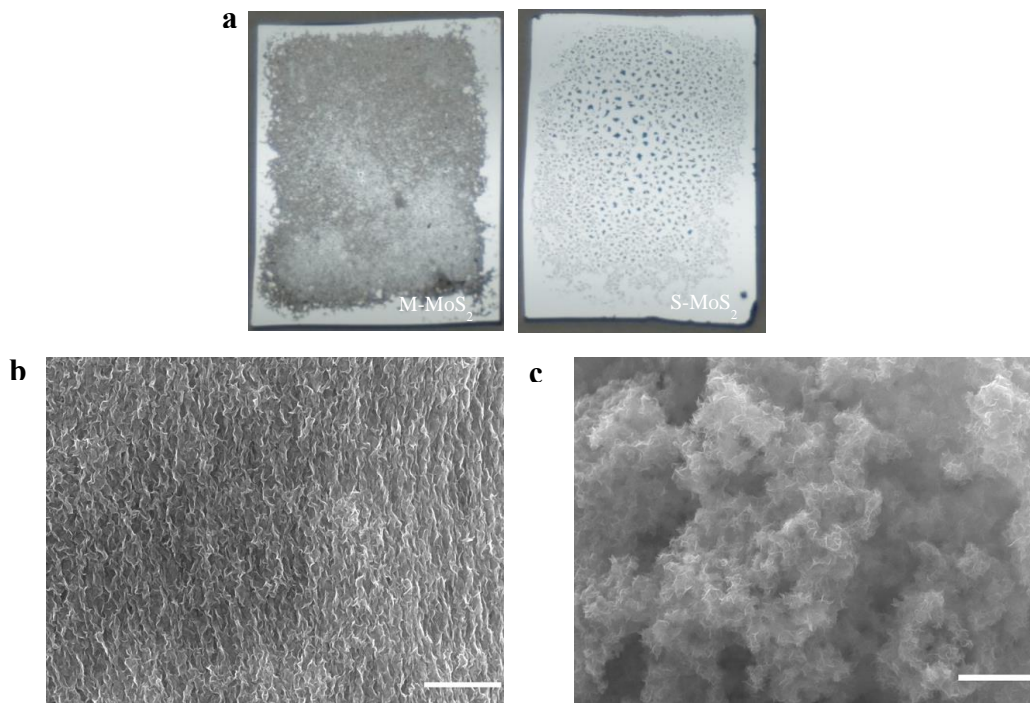


**Supplementary Figure 4: TEM images M-MoS<sub>2</sub> nanosheets. (a) High magnification.**

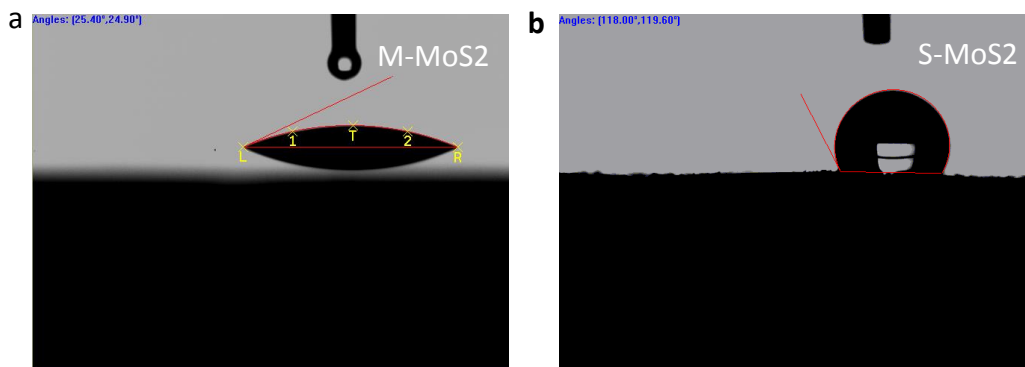
Scale bar, 2 nm. (b) Low magnification. Scale bar, 10 nm.



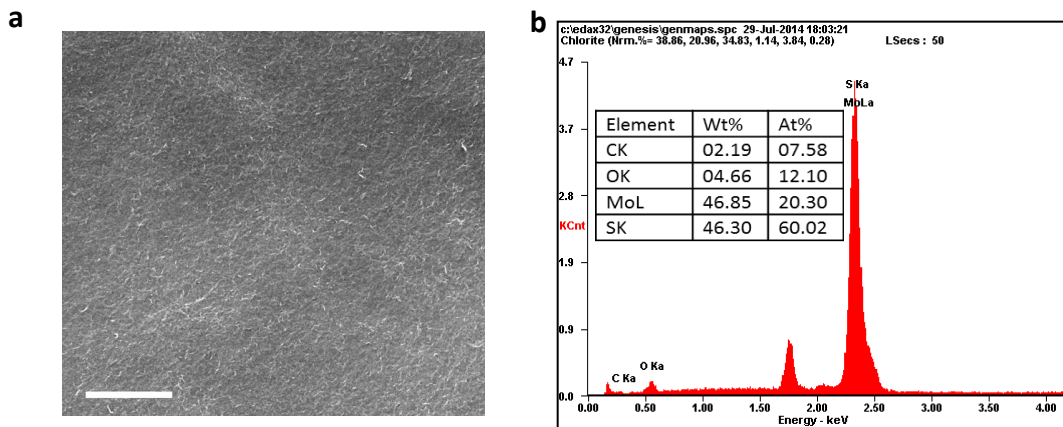
**Supplementary Figure 5: Raman spectroscopy of different samples.** (a) Fresh M-MoS<sub>2</sub> (Red). (b) 90-day-old M-MoS<sub>2</sub> stored in water (Pink), The M-MoS<sub>2</sub> sample stored for 90 days in water did not show obvious difference from freshly made M-MoS<sub>2</sub>, indicating that the M-MoS<sub>2</sub> nanosheets are very stable in water. (c) M-MoS<sub>2</sub> film (Black). The M-MoS<sub>2</sub> films after drying for 5 hours in vacuum show an obvious peak at 378 cm<sup>-1</sup>, which suggests that a fraction of M-MoS<sub>2</sub> has changed into S-MoS<sub>2</sub>. (d) S-MoS<sub>2</sub> (Blue). Though the defects developed in air may affect the Raman features in terms of peak position and width, they would not affect the conclusion drawn from the Raman whether or not the material is metallic.



**Supplementary Figure 6: Film morphologies of M-MoS<sub>2</sub> and S-MoS<sub>2</sub>.** (a) Optical images of the M-MoS<sub>2</sub> and S-MoS<sub>2</sub> on silicon substrates. (b and c) SEM images of M-MoS<sub>2</sub> and S-MoS<sub>2</sub> films. Scale bar, 1  $\mu\text{m}$ .

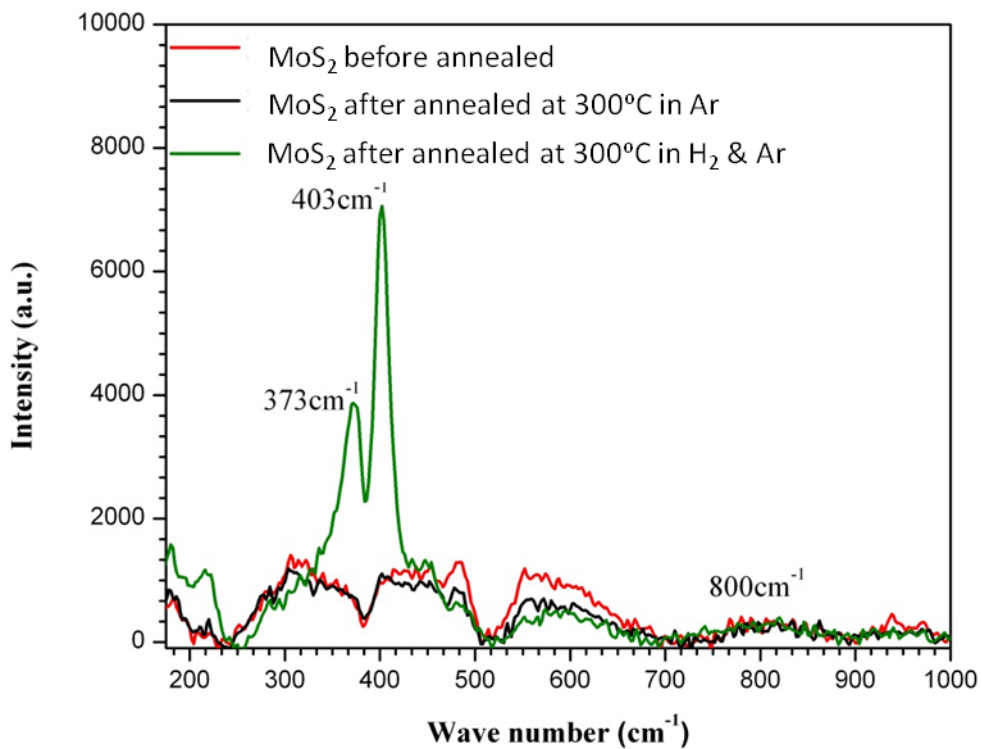


**Supplementary Figure 7: Static contact angle images.** (a) Fresh M-MoS<sub>2</sub> film. We measured the contact angle by drop casting a droplet of water (5  $\mu$ L) on the M-MoS<sub>2</sub> film and obtained an angle of 25°. (b) S-MoS<sub>2</sub> film. The same experiments were done on the S-MoS<sub>2</sub> films and an angle of 118° was found. These results confirm the hydrophilic surface of M-MoS<sub>2</sub> and hydrophobic surface of S-MoS<sub>2</sub>

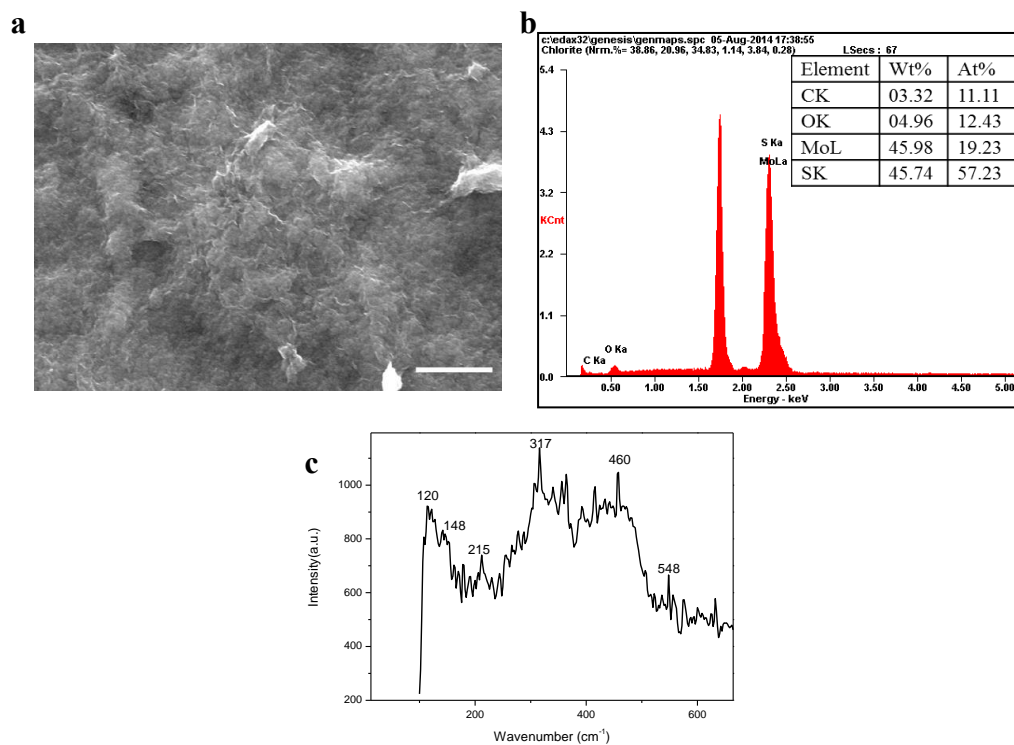


**Supplementary Figure 8: Characterization of MoS<sub>3</sub>.** (a) SEM image of amorphous MoS<sub>3</sub>. Scale bar, 1 μm. (b) EDX of MoS<sub>3</sub>.





**Supplementary Figure 9: Raman shift of MoS<sub>2</sub> before and after annealing in Ar and Ar/H<sub>2</sub> mixture.** MoS<sub>2</sub> before annealing (Red), MoS<sub>2</sub> after annealing at 300 °C in Ar (Black), MoS<sub>2</sub> after annealing at 300 °C in H<sub>2</sub> and Ar (Green),



**Supplementary Figure 10: Characterization of as-prepared intermediate phase  $\text{MoS}_3$ .** (a) SEM image of amorphous intermediate. Scale bar,  $1\ \mu\text{m}$ . (b) EDX result of intermediate and element ratio above. (c) Raman spectrum for samples prepared for one-and-a-half hours. The brown-black solution of  $\text{MoS}_3$  showed peaks at  $120\ \text{cm}^{-1}$ ,  $215$ ,  $317$ ,  $460\ \text{cm}^{-1}$  in Raman spectra. Meanwhile, a weak metal-metal peak located at  $146\ \text{cm}^{-1}$  was detected. Only a metal-metal Raman peak at  $146\ \text{cm}^{-1}$  was observed if the reaction was stopped after six hours (see Figure 1b).

## Supplementary Note 1

### XPS of M-MoS<sub>2</sub>

De-convolution of these peaks in XPS of M-MoS<sub>2</sub> reveals that the ratio of M-MoS<sub>2</sub> to S-MoS<sub>2</sub> is close to 6:1 (see Supplementary Figure 3). As a result, the M-MoS<sub>2</sub> content is estimated to be ~ 86% in the sample. However, this value does not reflect the content of the freshly prepared M-MoS<sub>2</sub>. The XPS was conducted at high vacuum for a few hours, during which some of the M-MoS<sub>2</sub> converts to S-MoS<sub>2</sub>. This phase transformation in vacuum was confirmed in our Raman measurements. Therefore, the Mo components associated with S-MoS<sub>2</sub> in XPS reflect the phase transformation of M-MoS<sub>2</sub> to S-MoS<sub>2</sub> in the vacuum chamber.

### Supplementary Discussion

#### Exchange current density

Exchange current density is the rate of reaction at the reversible potential. At the reversible potential, the reaction is in equilibrium, meaning that the forward and reverse reactions progress at the same rates. We have used the linear part of the polarization curve at small over-potentials in H<sub>2</sub>-saturated 0.5 M H<sub>2</sub>SO<sub>4</sub> solution to obtain  $j_0$  values. The exchange current density can be calculated by equation below.

$$\frac{\Delta j}{\Delta \eta} = j_0(nF/RT)$$

Here  $n$  represents the number of electrons exchanged,  $F$  (96485 C mol<sup>-1</sup>) is the Faraday constant, and  $R$  (8.314 J mol<sup>-1</sup>K<sup>-1</sup>) is the gas constant. The exchange current densities of 0.55, 0.1 and 0.04 mA cm<sup>-2</sup> were obtained for Pt, M-MoS<sub>2</sub> and S-MoS<sub>2</sub> from the polarization curves.

## **Supplementary Methods**

### **Preparation of MoS<sub>3</sub>**

12 mg MoO<sub>3</sub> and 14 mg thioacetamide were dissolved in 10 ml deionized water and stirred for two hours. The solution was added to the autoclave and then loaded into the furnace at 200 °C for twelve hours. After that, the reaction was stopped by rapidly cooling the solution down to room temperature. The yielded MoS<sub>3</sub> was collected and washed in deionized water several times. The as-prepared MoS<sub>3</sub> is amorphous structure as shown by SEM and the ratio of Mo to S is 1:3 as measured by EDX (Supplementary Figure 8).

### **Prepare S-MoS<sub>2</sub> by different procedure**

12 mg MoO<sub>3</sub>, 14 mg thioacetamide and 0.12 g urea were dissolved in 10 ml ethanol or dimethylformamide (DMF) and stirred for two hours. The solution was added to the autoclave and then loaded into the furnace at 200 °C for twelve hours. After that, the reaction was stopped by rapidly cooling the solution down to room temperature. The yielded small amount of precursor of S-MoS<sub>2</sub> was collected and washed in deionized water for several times. Then S-MoS<sub>2</sub> was obtained after the precursor was annealed at 300 °C under hydrogen flow of 50 sccm for one hour. Raman shifts show the highly crystalline structure of pure S-MoS<sub>2</sub> in Supplementary Figure 9. It was noticed that hydrogen plays an important role in reducing the precursor to S-MoS<sub>2</sub> since we found that MoS<sub>2</sub> is not produced if only Argon was used during annealing. If the solvent is a mixture of ethanol and water in a 1:1 ratio, no solid product was found in the autoclave, indicating that the type of solvent is important in the formation of MoS<sub>2</sub>.

### **Control experiment of M-MoS<sub>2</sub>**

12 mg MoO<sub>3</sub>, 14 mg thioacetamide and 0.12 g urea were dissolved in 10 ml deionized water and stirred for two hours. The solution was added to the autoclave and then loaded into furnace at 200 °C for one-and-a-half and six hours, respectively. After that, the reaction was stopped by rapidly cooling the solution down to room temperature. The yielded solid materials were collected and the ratio of Mo to S was found to be close to 1:3 when the reaction was stopped after one-and-a-half hours. The amorphous structure was characterized and shown in Supplementary Figure 10.